Journal of Renewable Energies 27 (2024) 339 – 358

DOI: https://doi.org/10.54966/jreen.v27i2.1308

Journal of Renewable Energies

Revue des Energies Renouvelables

journal home page: https://revue.cder.dz/index.php/rer

Research paper

Investigation on Syngas production from forest Biomass (Sapele, Sypo and Ayous) wood in the downdraft gasifier using Aspen plus and IC engine integration

Daivy Dieu-Le-Veut Djimbi Makoundi [a,*], **Lei Zhang** [b]

[a] *Hebei Key Laboratory of Low Carbon and High Efficiency Power Generation Technology, North China Electric Power University, Baoding 071003, Hebei, China*

[b] *School of Energy and Power Engineering, North China Electric Power University, Baoding 071003, Hebei, China*

ARTICLE INFO

Article history:

Received October 30, 2024

Accepted December 12, 2024

Keywords:

Sapele,
Sipo,
Ayous,
Downdraft gasification,
IC engine syngas integration.

ABSTRACT

This study aims to evaluate the potential for syngas production from three types of equatorial forestry biomass Sapele, Sipo, and Ayous using a downdraft gasifier. The main objective is to assess the energy potential of the produced syngas when used in an internal combustion engine with a 30% efficiency, coupled with a DC generator operating at 93% efficiency. The research focuses on determining the composition and energy output of syngas from these biomass types, as well as exploring the integration of downdraft gasification with internal combustion engines for localized energy production, particularly in decentralized power systems and microgrids.

The research involved modeling and simulating the gasification process using Aspen Plus software. Proximate and ultimate analyses of the biomass samples were used to simulate gasification in a downdraft gasifier. The gasifier's performance was assessed through syngas composition analysis, focusing on energy output and overall system efficiency. The integration of downdraft gasification with an internal combustion engine was simulated to determine its feasibility in decentralized power systems and microgrids.

The study revealed that all three biomass types produced syngas with high concentrations of carbon monoxide (CO) and hydrogen (H_2), which are critical for energy generation. The lower heating value (LHV) of the syngas remained consistent among the samples, with Sapele at 13.51 MJ/Nm³, Sipo at 13.63 MJ/Nm³, and Ayous at 13.54 MJ/Nm³. Ayous achieved the highest gasification efficiency at 79.36%, followed by Sipo at 78.89% and Sapele at 76.05%. The simulation performed in Aspen Plus showed that Ayous produced the highest electric power output at 53.55 kW, followed by Sapele at 51.86 kW and Sipo at 49.18 kW.

The results highlight the potential of equatorial forestry biomass, particularly Ayous, as a renewable energy source. All three biomass types can generate syngas of comparable quality in terms of energy content, with Ayous showing the highest efficiency. This research emphasizes the feasibility of using equatorial biomass for syngas production and its integration into internal combustion engines, supporting decentralized energy generation and reducing reliance on fossil fuels.

[*] *Corresponding author, E-mail address: 120204300006@ncepu.edu.cn*
Tel : + 8618830271115

ISSN: 1112-2242 / EISSN: 2716-8247

1. INTRODUCTION

Having driven the industrial revolution, fossil fuels have long been the primary energy source due to their high energy efficiency. However, the growing global energy demand, depletion of fossil resources, and environmental impacts caused by greenhouse gas emissions have significantly increased the need for renewable energy sources such as wind, solar, and biomass. Among these, biomass stands out as a particularly promising renewable energy source (Shahzad, 2012) (Stolarski, 2021), especially in equatorial forest regions rich in lignocellulosic resources. Biomass is abundant and has the advantage of a zero carbon footprint (CO_2) because the CO_2 produced during the combustion of wood is equivalent to the CO_2 consumed during its growth (Velvizhi, 2022). Biomass primarily consists of forest residues, agricultural waste, and by-products from logging activities. This resource holds tremendous potential for energy production, particularly through technologies such as gasification, The thermochemical valorization of biomass through gasification enables the conversion of solid biomass into a synthesis gas composed mainly of CO, H_2, and CH_4 by employing an oxidizing agent such as air, oxygen, or steam (Tabish, 2021). The resulting syngas can be directly used to power internal combustion engines, providing a flexible and efficient method for electricity generation figure 1. This integration is particularly advantageous in decentralized power systems and microgrids, where reliable and sustainable energy sources are needed, reducing dependence on fossil fuel, and contributes to local economic development.

This energetic valorization process has recently attracted the attention of numerous researchers around the world (Braghiroli, 2020) (Nakomcic-Smaragdakis, 2016) (Yang, 2017), highlighting the environmental and economic advantages of the valorization of forest solid biomass in a thermochemical manner. Modeling and simulation of the gasification process are therefore fundamental steps in Industrial process analysis to enables the performance prediction of the different effects and variables that may intervene during the gasification stages. Thereby allowing the estimation of the composition and quantity of gas at the outlet of the gasifier according to the Ultimate and Proximate data of the biomass used as fuel, minimizing development costs by virtually simulating models (Zhang, 2024), evaluating energy production or raw material consumption, improving efficiency by maximizing production while reducing losses, and waste production. In this study, a simulation model was developed using Aspen Plus to evaluate the characteristics of solid biomass gasification for three equatorial forestry biomasses Sapele(A), Sipo(B), and Ayous(C) in a downdraft gasifier.

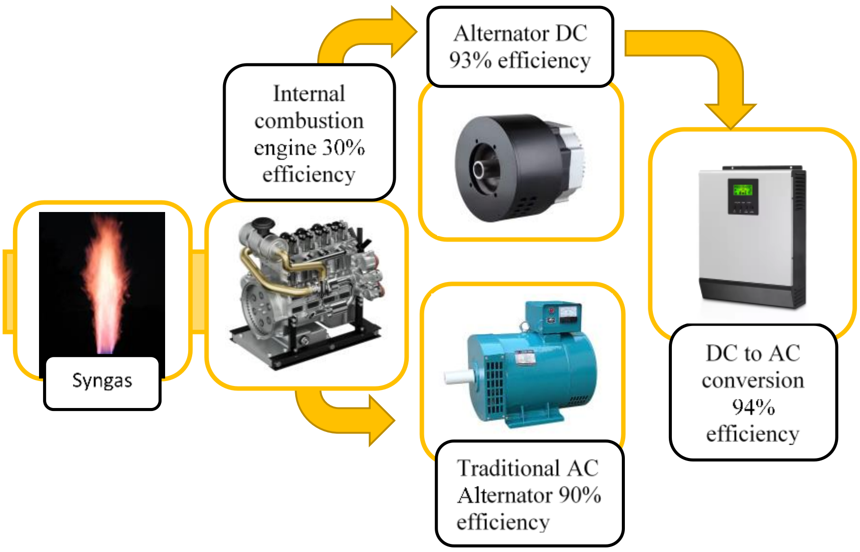

Fig 1. Integration of syngas in IC engine

The objective was to determine the energy potential of the produced syngas when used in a 30% efficiency internal combustion engine coupled with a DC generator of 93% efficiency. The investigation focused on the syngas composition, energy output, and overall system efficiency, emphasizing the integration of downdraft gasification syngas into internal combustion engines as a viable solution for local energy production.

1.1 Previous works

In recent decades, the focus has shifted towards integrating biomass gasification with IC engines for power generation, particularly in remote or rural areas where access to conventional energy sources is limited. Studies by (Kohli, 2003) and (Malik, 2013) demonstrated that gasification-IC engine systems could provide reliable electricity for small communities, utilizing locally available biomass resources. These systems were shown to have lower emissions and higher efficiency compared to traditional biomass combustion methods. A. Visconti has simulated the lingo cellulosic biomass pyrolysis based on equilibrium and main process ranking variables showing the main limiting assumption of the model developed to reach thermodynamic equilibrium by the comparison of the predicted result and some experimental reference (Visconti, 2015). With experimental results on Pine Kernel Shell in the fluidized bed reactor María Pilar González-Vázquez has developed an equilibrium model based on stoichiometric and minimization of Gibbs Free Energy using Aspen Plus®, to predict and compare the gas composition during biomass gasification Aspen Plus® (Pilar González-Vázquez, 2021). Gagliano developed an equilibrium model using Aspen Plus®, which is based on methanation and water-gas shift, to simulate the biomass gasification process in a downdraft gasifier considering char and tar formation, and the results showed good agreement between the experiment and data (Gagliano A. N., 2017). Gagliano developed a robust numerical model based on the downdraft gasification process to simulate the characterization of syngas composition, showing the relationship between the low heating value, temperature, and moisture content (Gagliano A. N., 2016). Sharmina Begum has carried out a numerical investigation of the gasification process on municipal solid waste using Aspen Plus. The fixed-bed gasification model is based on the Gibbs free energy minimization approach, which allows a long range of operating conditions (Begum S. R., 2014).

On Aspen Plus Roque Alguado performed simultaneous renewable electricity production using wet biomass, using a mini turbine associated with drying stages the simulation achieved a satisfactory result of 51,0% electricity efficiency on the dry stage sample (Fernández-Lobato, 2022). Thermogravimetric and kinetic analyses are parameters that make it possible to determine the composition and quality of different biomass to and estimate in which field of application it can be used, Xiao has carried out the kinetics pyrolysis study on lignocellulosic biomass to elucidate the characteristics of biomass pyrolysis (Xiao, 2020).

1.2 Method

The work consisted of modeling the gasification of three equatorial forest biomass samples Sapele, Sipo, and Ayous using Aspen Plus software. Using the proximate and ultimate data, the simulation model reproduces the key stages of downdraft gasification: pyrolysis, oxidation, and reduction. By applying thermodynamic models, the gasification reactions were modeled to achieve optimal syngas production conditions, including the separation of syngas and solid residues for data collection. The integration of the produced syngas with an internal combustion engine was simulated to assess the energy potential, considering an engine efficiency of 30% and a generator efficiency of 93%. The power outputs were calculated based on the syngas composition and its lower heating value (LHV). Despite some simplifications, the methodology provides a detailed framework for understanding and optimizing biomass gasification for energy production.

2. DOWNDRAFT GASIFIER

Three primary types of gasification technologies are widely used figure 2, Entrained Flow, Fluidized Bed, and Fixed Bed gasifiers. Each technology has unique characteristics, making them suitable for different scales and applications in power generation. Among the different gasification technology, fixed-bed downdraft gasification is attractive because it is relatively simple and robust, ideal for small-scale applications, particularly in rural or isolated contexts, where it can generate energy from local resources such as wood or agricultural waste. Due to its simplicity and reduced costs, it is well-suited for decentralized projects and micro grids.

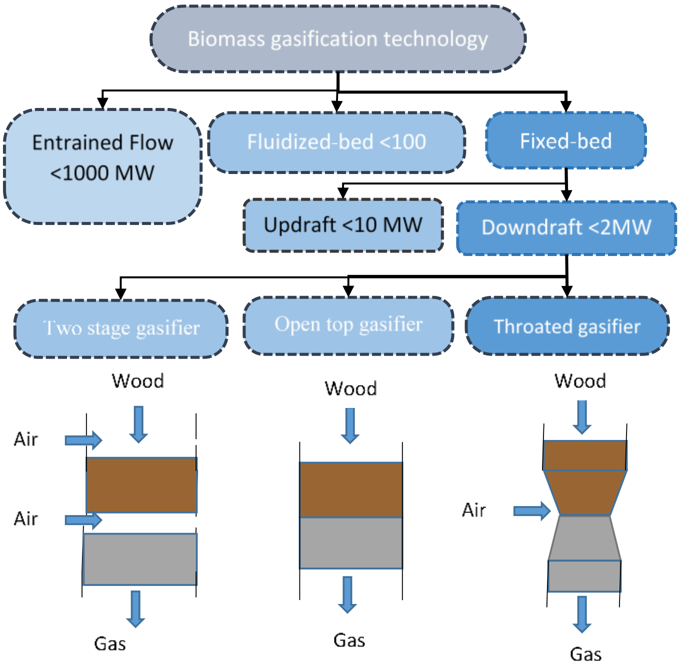

Fig 2. Gasification of syngas in IC engine

In a Fixed-bed gasification biomass moves vertically and forms a dense bed within the reactor, thus making it possible to operate at extremely high temperatures and flows, allowing rapid conversion of the material with a residence time in the combustion chamber of a few seconds. Thus making it possible to obtain carbon conversions on the order of 98 to 99.5% (Begum S. R., 2013). Biomass is devolatilized "Eq. (1)" through different stages of drying, pyrolysis, combustion, and reduction. Carbon, which is the main component of wood, reacts with the oxygen and steam in the gasifier to form carbon monoxide and hydrogen.

$$C_xH_yO_z = gC + hC_2O + aCH_4 + eH_2 + fCO + bCO_2 \tag{1}$$

During the downdraft process as is describe in figure 3, the air injection zone is generally designed to restrict the entry of air into the reactor, which promotes the oxidation of volatile materials. Gas is produced through the oxidation zone at a high temperature, which promotes thermal cracking of the tars while reducing the tar content present in the gas. Biogas can thus be used in an electric generator for the production of electricity, hydrogen, converted into chemicals or liquid fuels using different processes such as the Fischer-Tropsch (FT) process (dos Santos, 2020).

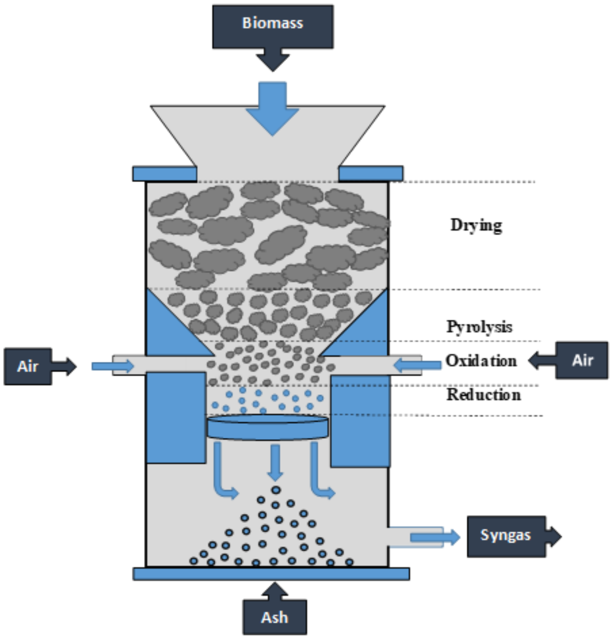

Fig 3. Downdraft Gasifier

Table 1. Chemical reactions in biomass gasification

Gasification step	Reactions		ΔH˚(KJ.mol-1)
Pyrolysis	Biomass → Char + Tar + Volatiles		
Oxidation	$Char(s) + O_2 \rightarrow CO_2$	Carbon oxidation	-394
	$C(s) + 0.5O_2 \rightarrow CO$	Carbon partial oxidation	-110
	$CO + 0.5O_2 \rightarrow CO_2$	Carbon monoxide oxidation	-283
	$H_2 + 0.5O2 \rightarrow H_2O$	Hydrogen oxidation	-242
Reduction	$C(s) + CO_2 \leftrightarrow 2CO$	Boudouard reaction	172
	$C(s) + H_2 O \leftrightarrow CO + H_2$	Reforming of char	131
	$CO + H_2 O \leftrightarrow CO2 + H_2$	Water gas shift reaction	-42
	$C(s) + 2H_2 \leftrightarrow CH_4$	Hydrogasification	-75
	$CH_4 + H_2O \leftrightarrow CO + 3H_2$	Steam-methane Reforming	206

In gasification processes, the materials used as fuel and the gasifier configurations have a significant impact on gas production. The chemical reactions that often occur in biomass gasification processes are summarized in table 1.

3. EXPERIENCE DATA AND BIOMASS MATERIAL

The biomass model simulates the gasification of three different biomass samples based on ultimate and proximate analysis data, which were obtained from previous research, where the Kinetic and Thermodynamic Parameters of the tree equatorial wood sample from the forests of Congo Brazzaville forestry Sapele(A), Sipo(B), and Ayous(C), are presented in Table 2.

For the purpose of the simulated model, the assumption that the particle size distributions shown in Figures 4 and 5 have been included to provide complete data on the PSD particle size distribution mesh, where solid Biomass and Ash are less than 20 mm for Sapele(A), Sipo(B), and Ayous(C).

Table 2. Proximate and ultimate Analysis of Sapele (A), Sipo (B) and Ayous (C)

Parameter	**A**	**B**	**C**
Proximate analysis (wt %)			
Fixed moisture	3,93	4,63	4,07
Volatile matter	79,93	81,95	80,79
Ash content	1,94	1	2,1
Fixed carbon	14,2	12,42	13,04
Ultimate analysis (wt %)			
Carbon	47,27	47,31	47,27
Hydrogen	5,57099999	5,96300000	6,077
Nytrogen	0,14000000	0,15	0,42
Sulfur(soufre)	4,25	1,605	0,58299999
Oxygen	40,82900001	44,972	44,133

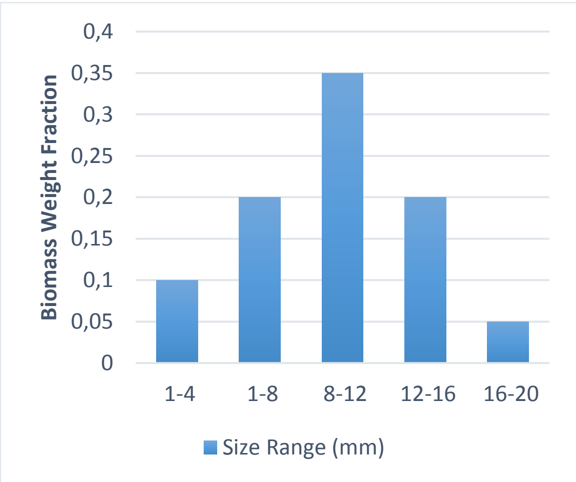

Fig 4. Biomass particle size distribution

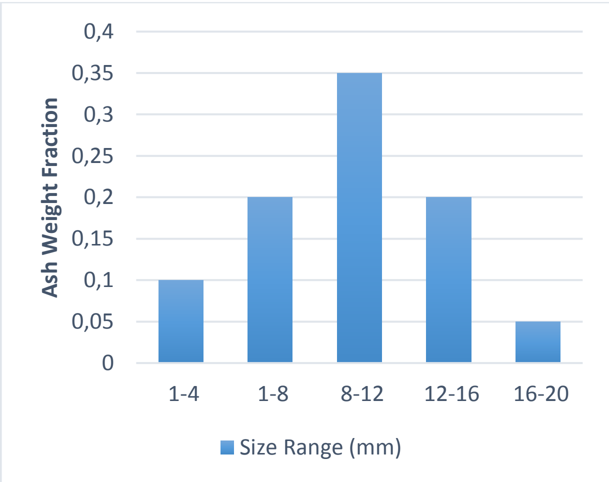

Fig 5. Ash particle size distribution

3.1 Engine power output using producer gas

Three different syngas compositions were analyzed to assess their suitability in a 30% efficiency IC engine coupled with a DC generator of 93% efficiency, when the capacity of the IC engine has selected accordingly to the gas parameter such as gas flow and stoichiometric mixture LHV. The LHV of the syngas was determined by summing the contributions of each combustible component, adjusted for their specific energy content per kilogram:

$$\text{LHVa=i=1n Molar Flow Ratei} \cdot \text{LHVi} \tag{2}$$

The LHV per unit volume is then obtained by:

$$\text{LHV per unit volume} = \frac{\text{Total LHV}}{\text{Total syngas volume}} \tag{3}$$

The results provided the LHV per cubic meter of syngas, which is crucial for engine performance analysis. The total volume of syngas produced was calculated using the ideal gas law, which is given by:

$$\text{Volume} = \frac{\text{Mole} \cdot \text{R} \cdot \text{T}}{\text{P}} \tag{4}$$

Where *R* is the gas constant, T the temperature in Kelvin, and P the pressure in atmospheres. The volumes for hydrogen, carbon monoxide, and methane were computed based on their respective molar masses and measured mass flow rates.

The stoichiometric air-to-fuel ratio was calculated to ensure complete combustion, incorporating the oxygen requirements for each component:

$$\text{Total } O_2 = 0{,}5 \cdot \text{Moles } H_2 + 0{,}5 \cdot \text{Moles CO} + 2 \cdot \text{Moles } CH_4 \tag{5}$$

The theoretical mechanical power output was estimated using the engine's thermal efficiency:

$$\text{Mecanical Power} = \frac{\text{LHVmixture} \cdot \text{Volumemixture} \cdot \text{Efficiency}}{3{,}6} \tag{6}$$

Using an alternator with 95% efficiency, the electrical power output was calculated by:

$$\text{Electrical Power} = \text{Mecanical Power} \cdot \text{Alternator Efficiency} \tag{7}$$

4. MODELING OF BIOMASS GASIFICATION SYSTHEM AND IC ENGINE INTEGRATION

A model of a downdraft fixed-bed biomass gasifier using air as the fluidizing agent was developed using Aspens Plus. The model can simulate and predict in a short time the performance of downdraft gasifiers of different types of solid biomass, with the possibility of interacting with input data for different experimental conditions.

Figure 6 illustrates a downdraft gasification process, detailing the successive steps of material processing. The process begins with the introduction of a feed material flow of 50 kg/h at an initial temperature of 30°C and a pressure of 1 atm. This material first undergoes drying, where its temperature is raised to 150°C while maintaining the pressure at 1 atm, in order to remove the moisture present. Next, the dehydrated material moves to the decomposition stage, where it is heated to 500°C under the same pressure of 1 atm, allowing for the thermal degradation of volatile components. This process is followed by pyrolysis, where the material is subjected to a temperature of 700°C at 1 atm. This step is crucial for converting the material into gas, solid (charcoal), and tar. The products resulting from pyrolysis are then directed to a cyclone, where the solid is separated from the other components at a temperature reduced to 300°C, still under 1 atm. The remaining flow, containing tar and gases, is then cooled to 40°C at 1 atm in a separator, where the tar is extracted from the gases. The final products of the process are gas, solid (charcoal), and tar. The gas can be used as an energy source or for other chemical applications. The diagram also indicates the air flow conditions in the system, with an oxygen

(O_2) input of 21%, under a pressure of 1 atm and an initial temperature of 30°C, which is then preheated to 120°C. The air flow required for complete combustion is determined by the following formula: 0.5 × (MC-MH-MO_2) / 0.21, where M refers to the mass of the molecular components of the material.

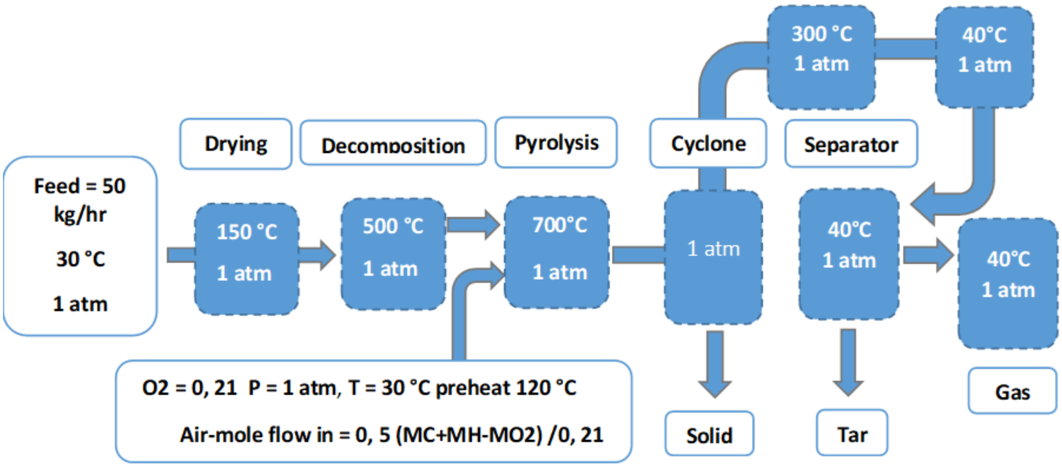

Fig 6. Gasification process flowchart

For IC engine integration illustrated in Fig 7 Air are firstly, preheated to 459°C and pressurized to 20 bar, along with biogas derived from syngas production, is introduced into the cylinder in a stoichiometric ratio. Inside the cylinder, this mixture undergoes combustion at a high temperature of 1500°C under a pressure of 1 atm. The energy released during combustion is then transferred to the crankshaft, which converts this thermal energy into mechanical work, capable of powering machinery or generating electricity. Finally, the exhaust gases produced from the combustion are expelled from the cylinder at 1 atm pressure, completing the cycle.

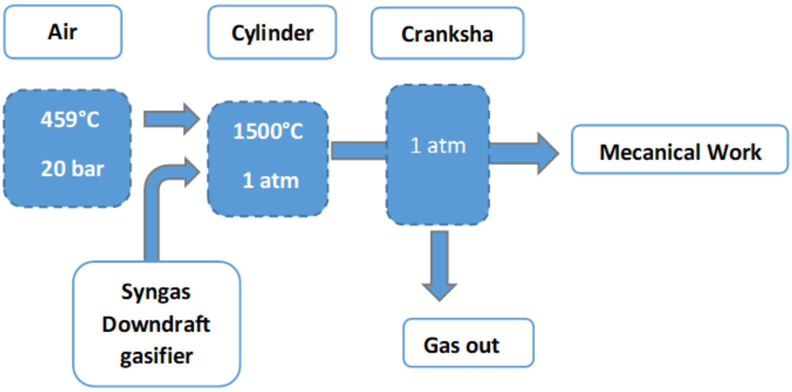

Fig 7. IC engine integration flowchart

Proximate and ultimate analysis data of the different biomass feedstock used in this simulation. According to ultimate and proximate analysis, non-conventional components have been defined. Figure 6 and 7 shows the model overview of the schematic simulation model and thermodynamic state for different stage.

The gasification simulation has been set in seven stages for the modeling of the entire gasification process. To simulate the equation of steam, PENG-ROB has been us as the method filter, HCOALGEN and DC HARRIGT to estimate enthalpy and density. The first stage is the drying stage, in which the moisture content in the biomass is reduced in the Rstoic reactor. In the second stage, by specifying the yield fraction distribution in the Ryield reactor using ultimate and proximate analysis data, the biomass feed is decomposed into elements. In the third stage, the RGibbs reactor was used to simulate the chemical equilibrium phase. In the Fourth stage, syngas and solid particles are separated using the cyclone. The fifth and sixth stages are cooling processes, where the hot steam gas is first cooled by bay air and finally cooled by water to reduce the temperature to ambient temperature.

The seventh stage is the liquid-gas separation process. Figure 8 shows the main flow sheet of the biomass gasification model and the IC engine integration where biomass is decomposed into the main elements such as Ahs, H2, CO, CO2, N, CH4. In the drying block, all biomass yield products are specified. The decomposition block predicts biomass decomposition into reference components at a fixed pressure and temperature. The equilibrium blocks Gibbs Free Energy minimization phase have been us to estimate the thermodynamic equilibrium.

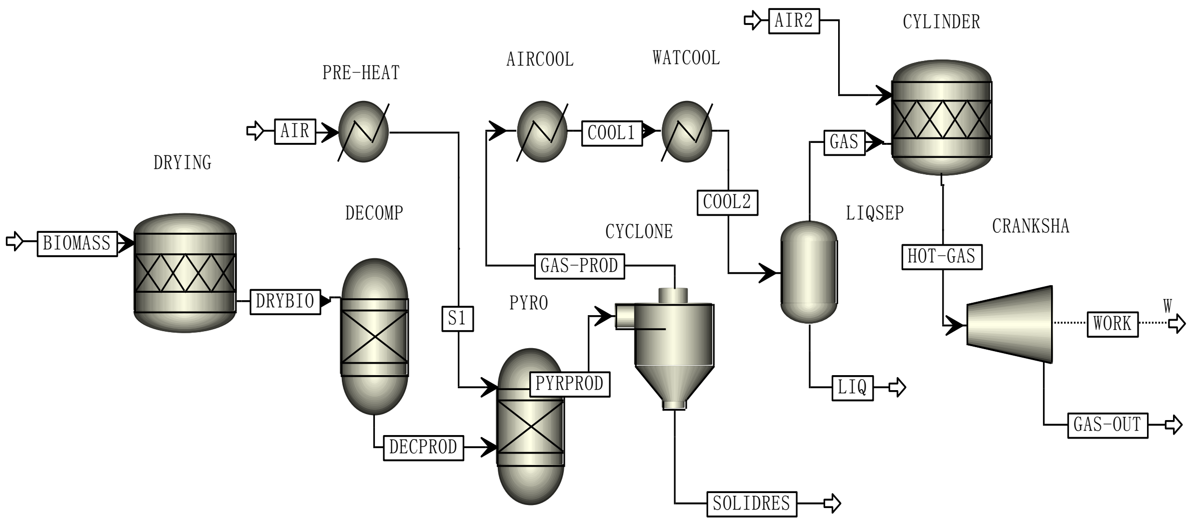

Fig 8. Aspen plus flowchart simulation

Higher quality gas is required for syngas IC engine integration, Tar Content < 50 mg/Nm³ (Mukunda, 1994), (Hernández, 2013). Rstoic reactor have been us to simulate the air fuel mixture combustion in the cylinder and the compressor have been us to simulate the conversion of thermal energy, generated from the combustion of the syngas-air mixture, into mechanical work in the crankshaft

5. RESULT AND DISCUSSIONS

In explaining the trend observed in Fig 4, a well-known reaction can accrue for the three samples Ayous (A), Sapele (B), and Sipo(C). The oxidation of carbon (C) to carbon dioxide (CO_2) in the presence of oxygen (O2) is a common form of combustion. This is represented by the following chemical reaction equation: $C+O_2 \rightarrow CO_2$. The water gas shift reaction known as (WGS) reaction, is a chemical reaction involving carbon monoxide (CO) and water vapor (H_2O) to produce carbon dioxide (CO_2) and hydrogen gas (H_2). This reaction is often represented by the following chemical reaction equation: $CO+H_2O \rightleftharpoons CO_2+H_2$.

We also observed a partial oxidation reaction of carbon (C) to form carbon monoxide (CO) the balanced equation for the reaction can be expressed as follows: 0,5 $O_2 \rightarrow CO$. CO_2+H_2 can also be obtained by endothermic reaction favored by the increase of temperature, where the consumption of H_2O, CH_4, and CO_2 gives H_2 and CO: ($C + H_2O \leftrightarrow CO + H_2$).

The formation of methane gas CH_4 can be due to the reaction of carbon C with hydrogen gas H_2, this reaction is known as Hydrogasification represented in is equation reaction as follows: $C+2H_2 \rightleftharpoons CH_4$.

Figures 9, 10 and 11 show the simulation results for the pyrolysis gas composition as a percentage for the three different wood feedstock species. In the Pyrolysis Reactor, the gas compositions of the three different feedstock were similar for Sapele(A) and Sipo(B). The high similarity observed between these three species is certainly due to their familiarity but also to the fact that they come from the same ecosystem. The gas produced by the pyrolysis reaction for all feedstock (A, B, C) is Mainly composed of Hydrogen (H_2) and Carbone dioxide (CO), these too elements are the main chemical elements present in the gas, and represent for them self-more than 88% of the final gas composition.

The remaining gas produced is not up to 7% and is composed of carbon dioxide (CO_2), hydrogen (H_2O), nitrogen (N_2), methane (CH_4), hydrogen, water, and carbon monoxide.

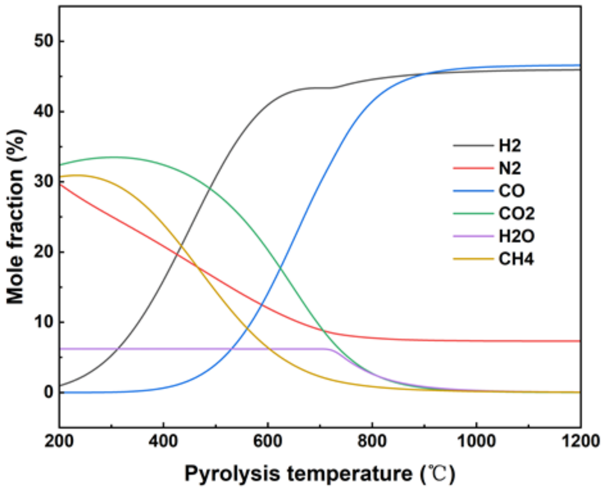

Figure 9. Sapele (A)

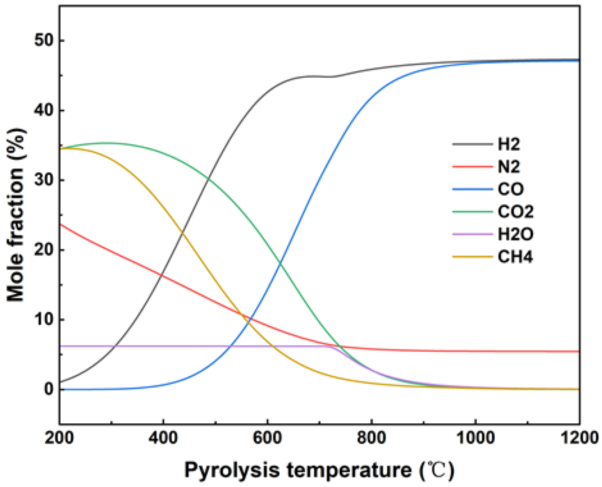

Figure 10. Sipo (B)

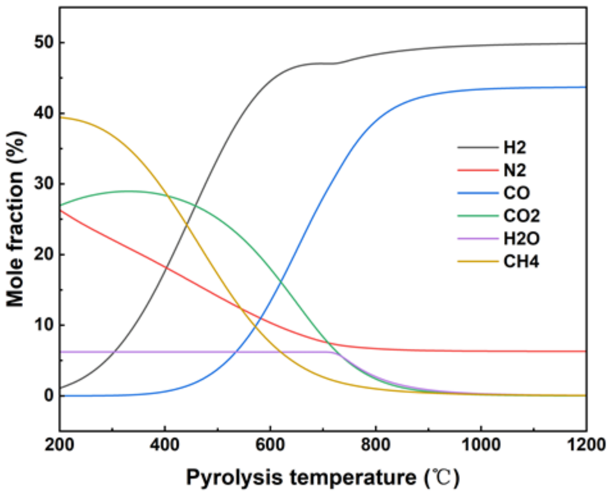

Fig 11. Ayous (C)

The concentrations of hydrogen H2, carbon dioxide CO, and hydrogen H_2O showed slight similarities across the three feedstock. At approximately 200 °C, a significant increase in the concentrations of carbon dioxide CO_2, nitrogen N_2, and methane CH_4 was observed. At 200 °C, Carbon dioxide CO_2 concentrations differed among feedstock 32% for A, 34% for B, and 24% for C.

The peak concentration was reached at 300°C for Sapele(A) and Sipo(B). 33% for Sapele(A) and 35% for Sipo(B), whereas Ayous(C) reached its peak at 350°C for 28% before decreasing. Feedstock B exhibited the highest percentage of hydrogen, surpassing A and C, when the H_2 concentration for A and B followed a similar increasing trend from 1% to 45% at 900 °C. Nitrogen (N2) concentration decreased for all feedstock 32% for Sapele(A), 23% for Sipo(B), and 26% for Ayous(C) before stabilizing at 800°C. At 200°C, Sipo(B) showed the highest methane CH_4 concentration of 32%, followed by Sapele(A) at approximately 32%, and Ayous(C) at the least 39%, before experiencing a decrease.

At 200°C, the water gas (H_2O) concentration was less than 6% for all the feedstocks, following a straight curve before an instant decrease of 75%. The reactions for hydrogen H_2 and carbon dioxide CO exhibit similarities for Sapele(A) and Sipo(B), with a key difference for Ayous (C).

At 200 °C, Sapele (A) and Sipo (B) showed a rapid increase in concentration, from 1% to 45% for Sapele (A) and 46% for Sipo (B). At 900°C for Ayou (C), the H_2 concentration was approximately 49%, and the CO concentration was 42% at the same temperature. The detailed analysis provides valuable insights into wood gas composition, emphasizing temperature-dependent variations and distinctions among different feedstocks. These findings are crucial for optimizing wood gas production processes and understanding the behavior of various feedstocks in pyrolysis chambers.

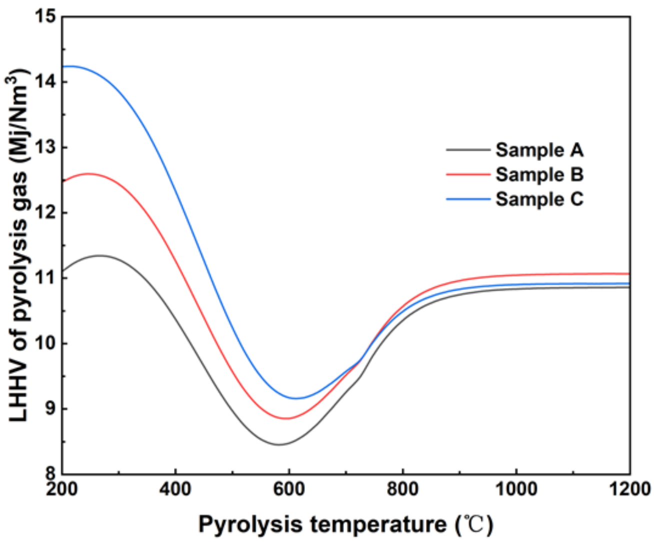

Fig 12. Pyrolysis LHV

Identifying the LHV (Lower Heating Value) of pyrolysis gases is crucial for the conversion of biomass into energy. Figure 12 illustrates the evolution of the LHV of pyrolysis gas for three different samples (A, B, and C) as a function of pyrolysis temperature in the combustion chamber, ranging from 200 °C to 1200 °C. A rapid drop in LHV for all samples is observed as the temperature increases from 200 °C to about 500 °C. This phase corresponds not only to the degradation of light volatile components but also to the reduction of chemical elements such as CH_4, CO_2, and N_2 in the syngas.

Sample A maintains the highest LHV across the entire temperature range, suggesting a composition rich in compounds that produce high-energy gas. Sample B shows intermediate performance, while Sample C displays the lowest LHV, indicating a potentially less favorable composition. After reaching a minimum at about 600 °C, the LHV of all samples tends to stabilize, which may indicate a slower decomposition phase of the remaining components.

The provided graph illustrates the evolution of the pyrolysis gas flow rate for Sapele (A), Sipo (B), and Ayous (C). Initially, all three materials show a gradual increase in gas flow from around 20 kg/h as the temperature rises from 200°C to 400°C, indicating the onset of thermal decomposition. Between 400°C and 800°C, the flow rate accelerates significantly, reaching a plateau of 50-55 kg/h, suggesting the completion of major pyrolytic reactions. The curves for Sapele, Sipo, and Ayous closely overlap, indicating similar pyrolytic behaviors, though Sipo consistently shows a slightly lower flow rate, and Ayous slightly higher, particularly at elevated temperatures.

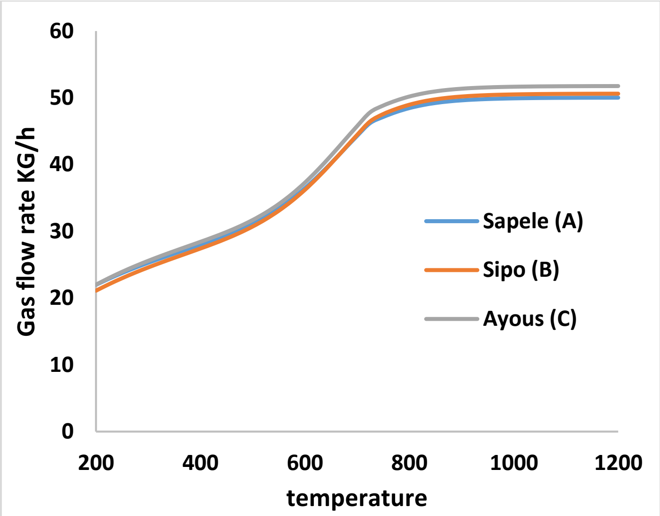

Fig 13. Pyrolysis gas flow rate kg/h

Understanding the dynamics of carbon content in relation to temperature is crucial due to the fundamental role that carbon plays in the combustion process and its direct impact on the heating value of the char produced. Figure 14 illustrates the relationship between pyrolysis temperature and the carbon content in char from three different wood feedstocks: Sapele(A), Sipo(B), and Ayous(C). As the pyrolysis temperature increases from 200°C to 1200°C, all three feedstocks show a decrease in carbon content. This trend is crucial because the carbon in the fuel is the primary source for energy generation during combustion. The higher the carbon content, the higher the potential energy (or heating value) of the char. Sipo (B) shows a steep decline in carbon content, decreasing from 97% at 200°C to about 90% at 800°C, and continuing to drop towards 85% by 1200°C. This indicates a rapid conversion rate of carbon, which might result in lower char yields but potentially higher gas yields at elevated temperatures.

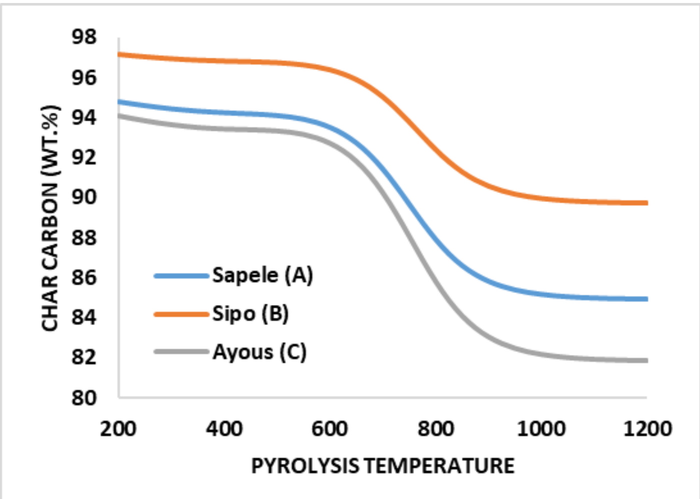

Fig 14. Carbon drop exhibition

Ayous(C) demonstrates a more gradual decline, beginning at 93% and reaching approximately 88% by 800°C, leveling off around 82% at 1200°C. This slower decline could mean a steadier char production rate. Sapele (A) mirrors the trend of Sipo (B) somewhat but with a slightly less steep decline, starting at 94% and reducing to around 89% at 800°C, and nearing 84% at 1200°C. This suggests a moderate balance between char stability and conversion efficiency. The pyrolysis temperature directly influences the carbon content in the char, which in turn affects the heating value. A higher pyrolysis temperature generally leads to a lower carbon percentage, decreasing the char's heating value but potentially increasing the volume and heating value of pyrolysis gases released. Selecting the optimal pyrolysis temperature and wood type depends on the desired balance between char production and gas production. For instance, Sipo might be preferable for processes where rapid gas production is desired, while Ayous could be better suited for applications needing a more controlled and prolonged char burning.

The figure 15 presents the output composition of various gases produced from the gasification process of Sapele , Sipo , and Ayous when the combustion chamber operates at 700°C and a water air cooling process at 40°C. The gases analyzed include water vapor H_2O, carbon monoxide CO, nitrogen N_2, hydrogen H_2, carbon dioxide CO_2, and methane CH_4.

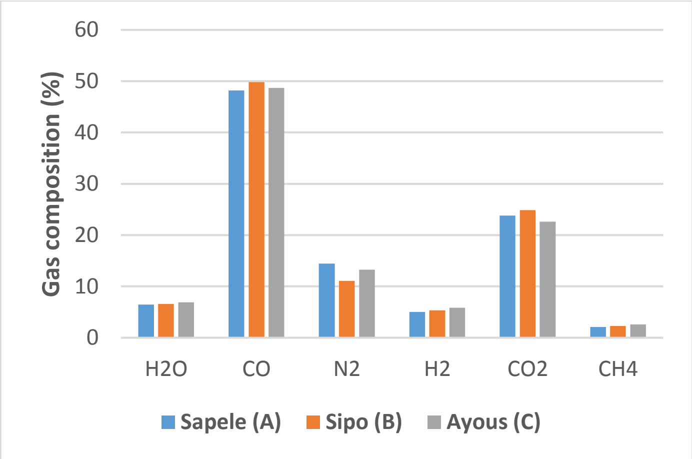

Fig 15. Output Gas composition for different biomass feed at 40 °C

The carbon monoxide production of CO is dominant across all three wood types, with Sipo (B) producing the highest percentage at approximately 49.85%, closely followed by Sapele at 48.68%, and Ayous at 48.18%. This high level of CO production is typical in pyrolysis processes due to the incomplete combustion of carbon materials. Carbone dioxide CO_2 percentages vary significantly among the woods. Ayous shows the highest CO_2 production at 24.86%, which might indicate a specific wood composition that facilitates CO_2 release, Sapele produces 23.82% and Sipo 22.63%. Nitrogen N2 percentages are notably higher in Sipo at 14.43%, compared to Ayous (13.29%) and Sapele (11.1%). This could be due to variations in the air flow. Hydrogen H2 and methane CH_4 are produced in smaller quantities. Sapele and Ayous generate slightly more H2 (5.86% and 5.33%, respectively) compared to Sipos 5.04%. Methane levels are low across all types, with Ayous producing the most at 2.63%, and Sapele and Sipo producing 2.27% and 2.08% respectively. These gases are typically produced in lesser amounts during pyrolysis due to the breakdown of more complex hydrocarbons. The production of water vapor is relatively consistent across the three types of wood, with Ayous producing slightly more (6.91%) compared to Sapele (6.59%) and Sipo (6.45%). This indicates similar moisture content in the woods, which can affect the overall gas composition.

Figure 16 illustrates the behavior of three types of wood (Sapele, Sipo, and Ayous) in a gasifier operating at 700 degrees Celsius, processing 50 kg/h of wood. Each type of wood is analyzed under four key aspects: gas flow output, solid residue output, air input, and tar residue output. For the gas flow output, Sapele and Sipo show comparable performance, both approaching 45%, while Ayous displays a slightly lower rate, near 42%. In terms of solid residues, Ayous is distinguished by a higher rate of about 15%, compared to Sipo and Sapele which produce about 12% and 10% respectively. This is due to differences in wood density from different samples which affects the amount of residue generated. The air input, which is critical for maintaining combustion and gasification, shows little variation between the woods, with Ayous having a slightly higher input, which can influence the efficiency of internal combustion. Finally, the output of tar residues is remarkably low for all types of wood, not exceeding 5%, with Ayous recording the lowest rate. This parameter is essential for assessing the quality of the produced gas and the need for cleaning gasification systems.

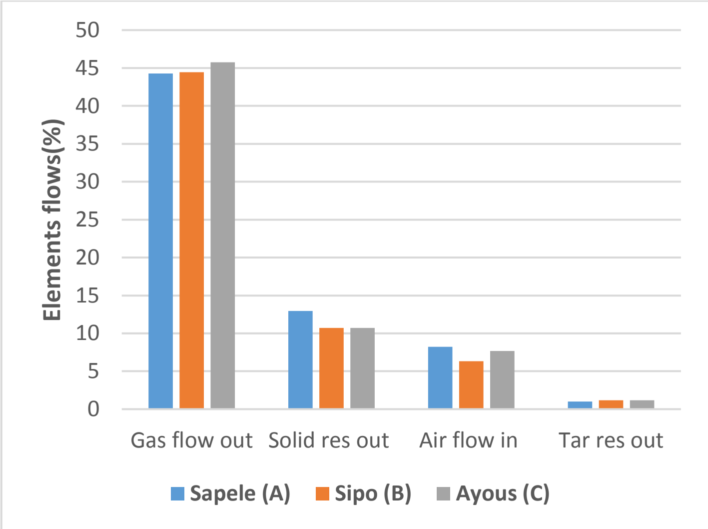

Fig 16. Gasifier element In-Out flows

The analysis of syngas production efficiency from different types of wood in the gasifier figure 17 reveals notable differences among the three woods studied. Ayous shows the best efficiency at about 79.36% is likely very effective in the pyrolysis and gas cooling stages, producing high-quality gas with minimal contaminants, making it the most optimal choice for maximal syngas conversion under the given conditions. Sipo follows with an efficiency of 78.89%, slightly lower than Ayous but still effective for syngas production.

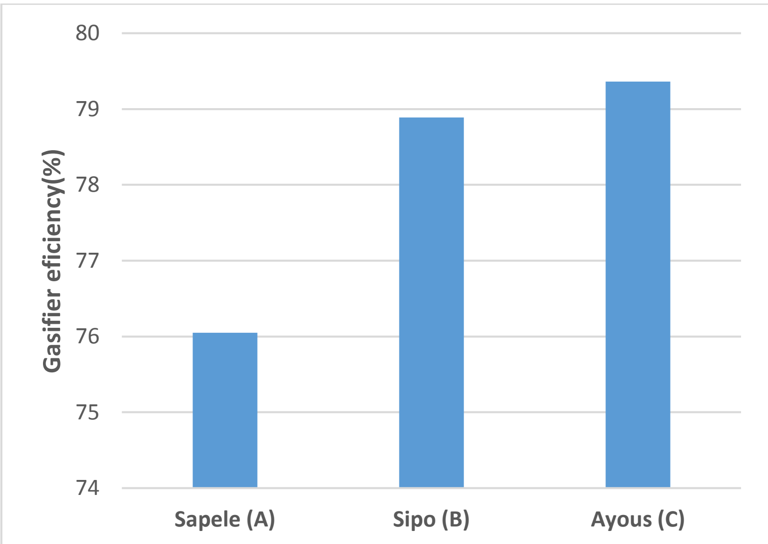

Fig 17. Syngas efficiency

Sapele presents the lowest efficiency at 76.05%, which may be due to intrinsic characteristics of the wood or variations in the gasification process. These results suggest that the choice of wood can significantly influence the efficiency of gasification. Therefore, to improve the overall performance of the gasification process, it would be prudent to consider adjustments in the choice of wood or in the process parameters for less efficient woods like Sapele.

The power generated by an engine running on producer gas is influenced by the same elements as engines using liquid fuels, specifically the heat content of the fuel and air mixture that enters the engine with each combustion cycle. The volume of the combustible mix that the engine takes in during each combustion cycle and the effectiveness with which the engine transforms the heat energy of the combustible mixture into mechanical energy (shaft power).

Table 3. IC engine Performance

Parameter	Sapele	Sipo	Ayou
Gas flow	42.75 kg/hr	42.85 kg/hr	44.05 kg/hr
Air flow	198.56 kg/hr	185.21 kg/hr	202.45 kg/hr
Horse Power	73.21 hp	69.41 hp	75.59 hp
Net Work	54.59 kw	51.76 kw	56.37 kw
DC Engin Electric Power output	51.86 kWe	49.18 kWe	53.55 kWe
65% efficiency AC Engin output	13.51 MJ/Nm³	13.63 MJ/Nm³	13.54 MJ/Nm³
LHV of stoichiometric mixture	13.51 MJ/Nm³	13.63 MJ/Nm³	13.54 MJ/Nm³

The performance of IC engines simulation fueled by syngas derived from these Sapele, Sipo and Ayous woods showed in table 3 revealing important insights into their efficiency and adaptability in energy production systems. Achieving complete combustion of syngas in internal combustion engines is critical for optimizing engine performance and minimizing environmental impact. The stoichiometric ratio, which defines the perfect balance of fuel to air that allows for complete combustion without excess, is essential in this context. This ratio depends on the specific components of syngas, typically hydrogen (H_2), carbon monoxide (CO), methane (CH_4), and carbon (C), each having distinct oxygen requirements for complete combustion.

Both hydrogen and carbon monoxide require half a mole of oxygen per mole of fuel to fully convert into water (H_2O) and carbon dioxide (CO_2), respectively $H_2+0.5O_2 \rightarrow H_2O$, $CO+0.5O_2 \rightarrow CO_2$. Methane, a more complex hydrocarbon, requires two moles of oxygen per mole to produce water and carbon dioxide $CH_4+2O_2 \rightarrow 2H_2O+CO_2$. Pure carbon combustion directly to CO_2 is a straightforward process requiring a one to-one mole ratio with oxygen $C+O_2 \rightarrow CO_2$. If there is an insufficient oxygen supply, carbon may only partially oxidize to carbon monoxide $O_2+C \rightarrow CO$.

For Sapele, the gas flow rate is recorded at 42.75 kg/hr with an air flow of 198.56 kg/hr. In comparison, Sipo has a slightly higher gas flow rate at 42.85 kg/hr but a lower air flow rate of 185.21 kg/hr. Ayou, on the other hand, exhibits the highest gas flow rate at 44.05 kg/hr and an air flow of 202.45 kg/hr. The conversion of syngas energy in horsepower (hp) and net work output further highlight the differences in performance across the three wood types. Sapele generates 73.21 hp and 54.59 kW of net work, while Sipo, with slightly lower values, produces 69.41 hp and 51.76 kW. Ayou again stands out with the highest figures at 75.59 hp and 56.37 kW.

There the net work power represents the conversion of horsepower in kW. However, the marginal differences between Sapele and Ayou indicate that Sapele could also be a viable option, particularly in systems where slightly lower output is acceptable. The conversion of mechanical energy to Electric power is another critical aspect, especially in systems where syngas is used to generate electricity. Sapele, Sipo, and Ayou produce 51.86 kW, 49.18 kW, and 53.55 kW of electric power, respectively. Ayou, with the highest electric power output, reinforces its position as the most efficient fuel source among the three. However, the relatively close values across all three wood types suggest that they all can be considered for syngas-based electricity generation, depending on specific system requirements.

The Lower Heating Value (LHV) data for the stoichiometric mixture of syngas derived from Sapele, Sipo, and Ayous woods are quite close, indicating that each type of wood provides a nearly consistent energy content when gasified. Specifically, the LHV values are 13.51 MJ/Nm³ for Sapele, 13.63 MJ/Nm³ for Sipo, and 13.54 MJ/Nm³ for Ayous. These values suggest that the syngas from these different biomass sources can deliver comparable energy potential for combustion processes in internal combustion engines.

6. ECONOMIC FEASABILITY ASSESSMENT

Table 4 present the economic feasibility of implementing a biomass downdraft gasification system integrated with an internal combustion engine for electricity generation.

The following assumptions and considerations were taken into account for the assessment:

The total capital cost for setting up the integrated gasification system, including all major components, is estimated at $23926. This includes the costs for the gasifier, cooling and cleaning equipment, filtration system, internal combustion engine, wood cutting machine, electric 3-wheeled vehicles for biomass transport, and installation and commissioning costs.

Assuming that the system will use free biomass obtained from local forestry operations, such as Sapele, Sipo, and Ayous, as feedstock. The biomass consumption rate is approximately 50 kg per hour, translating to 1.2 tons per day. Since the biomass is sourced as exploitation residues, the daily cost of biomass is considered 0$.

The LCOE represents the price at which electricity must be sold for the system to break even over its operational lifetime, including both capital and operational costs. Assuming a 15-year operational lifetime and a discount rate of 8%, the LCOE for Sapele, Sipo and Ayous is $0.0695 per kWh, $0.0733 per kWh and 0.0674 per kWh respectively

If electricity generated by the system is sold at a rate of $0.10 per kWh, contributing to the revenue from the system, where the annual operating costs for Sapele, Sipo and Ayou is 23,879.11/year, $23,689.13/year, $23,990.09/year respectively

The payback period is calculated based on the annual revenue from electricity sales, using 15% of the revenue to recoup the initial capital investment. The payback period without subsidies is estimated at approximately at 4 years and 3 months for Sapele, 4 years and 6 months for Sipo and 4 years and for Ayous.

If the system benefits from a 35% subsidy, which reduces the total capital cost from $23926 to $15551.90, resulting in a significantly shorter payback period of 2 years and 8 months for Sapele, 2 years and 10 months for Sipo and 2 years and 7 months for Ayous

The average cost of electricity from the grid in Congo is approximately $0.079 per kWh, which makes the biomass gasification system a competitive alternative for energy generation, with its LCOE either comparable or lower than the grid electricity cost.

Table 4. Economic feasibility assessment of IC Engin integrated gasification plant.

Iteam		Value	Unit
Performance parameters			
Biomass Consumption		50	kg/h
Total Lifetime Energy Production	Sapele	5,590,080	kWh
	Sipo	5,304,960	kWh
	Ayous	5,774,400	kWh
Economic Parameters			
Gasifier, Cooling, Cleaning, Filtration		2 417	USD
IC Engine		8 266	USD
Wood Cutting Machine		805	USD
2 Units of Electric 3-Wheeled Vehicles		2 438	USD
Installation and Commissioning		2 000	USD
Total Capital Cost Without Subsidy		23 926	USD
35% of Non-Refundable Subsidy		8 374.10	USD
Effective Capital Cost with Subsidy		15 551.90	USD
Biomass Feedstock Cost		0	USD
Labor Costs		17 352	USD/year
Routine Maintenance Cost		1 000	USD/year
Operating Cost	Sapele	23,879.11	USD/year
	Sipo	23,689.13	USD/year
	Ayous	23,990.09	USD/year
Total Lifetime Costs for 15 years		388,577.65	USD
Annual Revenue From Electricity Sales	Sapele	37,267.20	USD/year
	Sipo	35,366.40	USD/year
	Ayous	38,496.00	USD/year
Electricity Cost in Congo		0.079	USD/kWh
Results			
LCOE (Levelized Cost of Energy)	Sapele	0.0695	USD/kWh
	Sipo	0.0733	USD/kWh
	Ayous	0.0674	USD/kWh
Payback Period Without Subsidy	Sapele	4.29	years
	Sipo	4.51	years
	Ayous	4.14	years
Payback Period With 35% Subsidy	Sapele	2.69	years
	Sipo	2.84	years
	Ayous	2.59	years

7. CONCLUSION

This study aimed to evaluate the gasification potential of three equatorial forestry biomass samples Sapele (A), Sipo (B), and Ayous (C) using a downdraft gasifier coupled with an internal combustion engine for energy production. The research involved modeling and simulating the gasification process using Aspen Plus, focusing on syngas composition and overall gasification for energy need. The investigation revealed that all three types of wood are capable of producing syngas with a relatively consistent lower heating value (LHV), indicating the uniformity of energy content across different biomass sources. This syngas has shown significant promise in powering internal combustion engines with a noted efficiency of 30%, coupled with a DC generator efficiency of 93%.

The analysis revealed that all three biomass types produced syngas with a high concentration of carbon monoxide (CO) and hydrogen (H2), which are critical for energy generation. Sipo exhibited the highest CO concentration at approximately 49.85%, followed closely by Sapele at 48.68% and Ayous at 48.18%. The stoichiometric mixture LHV, an essential indicator of the syngas's energy content, was relatively consistent across the samples, with Sapele at 13.51 MJ/Nm³, Sipo at 13.63 MJ/Nm³, and Ayous at 13.54 MJ/Nm³. These values suggest that all three biomass types are capable of generating syngas of comparable energy quality.

Gasification efficiency varied among the biomass types, with Ayous achieving the highest efficiency at 79.36%, followed by Sipo at 78.89% and Sapele at 76.05%. The differences in efficiency are significant as they reflect the varying effectiveness of each biomass type in converting feedstock into usable syngas. Furthermore, the solid residue output was influenced by the density and chemical composition of the wood samples, with Ayous producing the highest amount of solid residue (15%), followed by Sipo (12%) and Sapele (10%). Temperature played a critical role in the gasification process, particularly in influencing the composition of the syngas and the carbon content of the char. As the pyrolysis temperature increased from 200°C to 1200°C, the carbon content in char decreased for all three samples, with Sipo showing the steepest decline, indicating a rapid conversion rate of carbon, which might result in lower char yields but higher gas yields at elevated temperatures. The study also explored the engine performance based on the produced syngas. Sapele exhibited 73.21 horsepower and a corresponding electric power generation of 51.86 kW illustrating robust performance suitable for moderate to high-demand applications. Sipo produced a lower horsepower of 69.41 with an electric power output of 49.18 kW positioning it as a viable option for less intensive energy applications. Ayous Demonstrated the highest horsepower of 75.59 kdfjW leading to an electric power output of 53.55 kW and out as the most efficient among the tested samples, ideal for high-demand energy production settings. The efficiency of converting biomass into syngas was quantitatively assessed, revealing that Ayous displayed the highest overall gasification efficiency 79.36%, followed by Sipo 78.89% and Sapele 76.05%. This efficiency is pivotal for evaluating the suitability of each biomass type for syngas production.

Covering capital costs, operational expenses, and the Levelized Cost of Energy (LCOE) the economic analysis demonstrates the financial viability of integrating a downdraft gasification system with internal combustion engines (IC engines) using Sapele, Sipo, Ayous syngas, highlighting the competitive potential of equatorial forestry biomasses against conventional grid electricity, with an LCOE ranging from $0.0674 to $0.0733 per kWh.

This research underscores the significant potential of equatorial forestry biomass as a renewable energy source, particularly in regions rich in Solid Biomass resources. The consistent syngas quality and relatively high gasification efficiencies suggest that these biomass types can effectively meet local energy demands while reducing dependence on fossil fuels and supporting local economic development.

NOMENCLATURE

IC	Internal combustion engine	PSD	Particle size distribution	LCOE	Levelized Cost of Energy
LHV	Lower Heating Value	atm	Atmosphere		
A	Sapele	hp	Horsepower		
B	Sipo				
C	Ayous				

REFERENCES

Begum, S. R. (2013). Performance analysis of an integrated fixed bed gasifier model for different biomass feedstocks. *Energies*, 6(12), 6508-6524.

Begum, S. R. (2014). A numerical investigation of municipal solid waste gasification using aspen plus. *Procedia engineering*, 90, 710-717.

Braghiroli, F. L. (2020). Valorization of biomass residues from forest operations and wood manufacturing presents a wide range of sustainable and innovative possibilities. *Current Forestry Reports*, 6, 172-183.

dos Santos, R. G. (2020). Biomass-derived syngas production via gasification process and its catalytic conversion into fuels by Fischer Tropsch synthesis. *International Journal of Hydrogen Energy*, 45(36), 18114-18132.

Fernández-Lobato, L. A. (2022). Biomass gasification as a key technology to reduce the environmental impact of virgin olive oil production: A life cycle assessment approach. *Biomass and Bioenergy*, 165, 106585.

Gagliano, A. N. (2016). A robust numerical model for characterizing the syngas composition in a downdraft gasification process. *Comptes Rendus Chimie*, 19(4), 441-449.

Gagliano, A. N. (2017). Development of an equilibrium-based model of gasification of biomass by Aspen Plus. *Energy Procedia*, 111, 1010-1019.

Hernández, J. J. (2013). Characterisation of tars from biomass gasification: Effect of the operating conditions. *Energy*, 50, 333-342.

Kohli, S. &.-2.-1. (2003). Biomass gasification for rural electrification: prospects and challenges. *SESI Journal*, 13(1-2), 83-101.

Malik, A. &. (2013). Biomass-based gasifiers for internal combustion (IC) engines—A review. *Sadhana*, 38, 461-476.

Mukunda, H. S. (1994). Gasifiers and combustors for biomass–technology and field studies. . *Energy for Sustainable Development*, 1(3), 27-38.

Nakomcic-Smaragdakis, B. C. (2016). Analysis of solid biomass energy potential in Autonomous Province of Vojvodina. *Renewable and Sustainable Energy Reviews*, 57, 186-191.

Pilar González-Vázquez, M. R. (2021). Thermodynamic analysis of biomass gasification using aspen plus: Comparison of stoichiometric and non-stoichiometric models. *Energies*, 14(1), 189.

Shahzad, U. (2012). The need for renewable energy sources. *energy*, 2, 16-18.

Stolarski, M. J.-Z. (2021). Solid biomass energy potential as a development opportunity for rural communities. *Energies, 14(12)*, 3398.

Tabish, A. N. (2021). Biomass waste valorization by acidic and basic leaching process for thermochemical applications. *Waste and Biomass Valorization*, 1-11.

Velvizhi, G. G. (2022). Valorisation of lignocellulosic biomass to value-added products: Paving the pathway towards low-carbon footprint. *Fuel*, 313, 122678.

Visconti, A. M. (2015). An Aspen Plus® tool for simulation of lignocellulosic biomass pyrolysis via equilibrium and ranking of the main process variables. *International Journal of Mathematical Models and Methods in Applied Sciences*, 9, 71-86.

Xiao, R. Y. (2020). Thermogravimetric analysis and reaction kinetics of lignocellulosic biomass pyrolysis. *Energy*, 201, 117537.

Yang, X. W. (2017). Thermal properties of biochars derived from waste biomass generated by agricultural and forestry sectors. *Energies*, 10(4), 469.

Zhang, W. G. (2024). Thermodynamic modeling and performance analysis on co-gasification of Chlorella vulgaris and petrochemical industrial sludge via Aspen plus combining with response surface methodology. *International Journal of Hydrogen Energy*, 55, 1037-1049.